PCCP

Geometric and electronic structure analysis of calcium water complexes with one and two solvation shells

Journal:	*Physical Chemistry Chemical Physics*
Manuscript ID	CP-ART-08-2020-004309.R1
Article Type:	Paper
Date Submitted by the Author:	12-Sep-2020

Complete List of Authors:	Ariyarathna, Isuru; Auburn University, Chemistry and Biochemistry Miliordos, Evangelos; Auburn University, Chemistry and Biochemistry

Geometric and electronic structure analysis of calcium water complexes with one and two solvation shells

*Isuru R. Ariyarathna and Evangelos Miliordos**

Department of Chemistry and Biochemistry, Auburn University, Auburn, AL 36849-5312, USA

AUTHOR INFORMATION

Corresponding Author

* E-mail: emiliord@auburn.edu

ABSTRACT:

Neutral and cationic calcium water complexes are studied by means of high-level quantum calculations. Both the geometric and electronic structure of these species is investigated. We study complexes with up to eight water molecules in the first solvation sphere of calcium $Ca(H_2O)_{n=1\text{-}8}^{0,+}$, and examine their stability with respect to $Ca(H_2O)_{n\text{-}k}@kH_2O^{0,+}$, where a number k of water molecules resides at the second solvation shell. For the cationic species, we find that five water molecules readily attach to calcium and the sixth water molecule goes to the second shell. The hexa-coordinated calcium core is restored after the addition of a seventh water molecule. For neutral species, zero-point energy corrections are critical in stabilizing structures with water ligands directly bound to calcium for up to six water ligands. The (one or two) valence electrons of Ca^+ and Ca are displaced gradually from the valence space of calcium to the periphery of the complex forming solvated electron precursors (SEPs). For example, in the ground state of $Ca(H_2O)_6^+$ one electron occupies an s-type diffuse peripheral orbital, which can be promoted to higher energy p-, d-, f-, g-atomic-type orbitals (1s, 1p, 1d, 2s, 1f, 2p, 2d, 1g, 3s) in the excited states of the system. Finally, we considered the effect of a complete second solvation shell using the $Ca(H_2O)_6^+@12H_2O$ cluster, which is shown to have significantly lower excitation energies compared to the $Ca(H_2O)_6^+$.

1. Introduction

Although studies on solvated electron systems have a history of two centuries, their chemical and physical properties are still poorly understood.[1] The studies on solvated electron systems have focused mainly on the ammonia and water solvents. NH_3 and H_2O force valence electron(s) to detach from the metal core and solvate in their cavities.[1] In ammonia, solvated electrons last for days before vanishing with the release of H_2, but in water their lifetime is about 300 μs.[2] Hence, macro-scale studies on solvated electrons have been carried out exclusively in metal ammonia solutions.

A dilute metal ammonia solution has a brilliant blue color consisting of ion-pairs formed by metal cations and solvated electrons.[1] As the metal concentration increases, the density of solvated electrons in the solution rises causing spin-pairing between solvated electrons.[3] At 0.1 mol% metal concentration, more than 90% of the solvated electrons are paired.[3] In the 1-8 mol% range of metal concentration, the blue solution transforms into a bronze-gold colored liquid metal with an increased electrical conductivity.[3] At the saturation limit (21 mol% metal) the conductivity of this liquid metal goes beyond that of liquid mercury.[3] The metal-like conductivity of the formed species is attributed to their structure: "free" electrons orbit around positively charged metal ammonia complexes.

Solid-state studies of such metal-ammonia or metal-water species are rare. Edwards reports that solid $Li(NH_3)_4$ shows superconductivity around 180-190 K.[3] Further Seel et al. identified $Li(NH_3)_4$ as the lowest melting point metal.[4] A comprehensive solid-state computational study which focuses $Li(NH_3)_4$ has been conducted by the Hoffman group.[5]

At the opposite end, several gas phase studies on metal-ammonia and metal-water complexes can be found in the literature. Among those, studies on $Al(H_2O)_n^+$,[6-10] $Na(H_2O)_n$,[11-19] and $Mg(H_2O)_n^+$ [20,21-33] are common. Some reports about $Na(NH_3)_n$,[13, 34, 35] $Mg(NH_3)_n^+$,[36, 37] $Sr(NH_3)_n^+$,[38, 39] $Sr(H_2O)_n^+$,[32, 38, 40, 41] $Ba(H_2O)_n^{0,+}$,[42, 43] and $Ca(H_2O)_n^+$ [32, 44, 45] are also available. Cationic alkaline earth metal-water complexes adopt either a $M(H_2O)_n^+$ or a $M(OH)(H_2O)_{n-1}^+$ structure. For example, when n=1−5 or n>14 $Mg(H_2O)_n^+$ is favored, but for n=6−14 $Mg(OH)(H_2O)_{n-1}^+$ is dominant.[21, 22] For n=6 both $Mg(H_2O)_n^+$ and $Mg(OH)(H_2O)_{n-1}^+$ have been detected in 1:6 ratio by Misaizu et al.[21] Sperry et al. found that deuterium substitution causes

$Mg(D_2O)_n^+$ to be the main structure for n=1-6.[41] Deuterium substitution can also determine the chief isomer of cationic Sr^+–H_2O clusters. According to Sperry et al., $Sr(H_2O)_n^+$ is dominant for n=1−4, while $Sr(D_2O)_n^+$ dominates for n=1−5.[41]

Calcium water clusters produced by laser evaporation and their photo-dissociation spectra have been recorded by Fuke and co-workers.[44] Their mass spectrum points to $Ca(H_2O)_n^+$ structures for n=1−4 or n>12, whereas $Ca(OH)(H_2O)_{n\text{-}1}^+$ has been identified exclusively for n=5−12. The isotopic substitution of hydrogen showed that $Ca(D_2O)_n^+$ persists for every n value including n=5−12. Therefore, they recorded the photo-dissociation spectrum of $Ca(H_2O)_n^+$ for n=1−5, but they used $Ca(D_2O)_6^+$ instead of $Ca(H_2O)_6^+$. These authors supported that the spectrum is not affected by the deuterium substitution since the $Ca(D_2O)_6^+$ fragments used to record the spectrum are hot and should be identical to that of $Ca(H_2O)_6^+$. Their photo-dissociation results suggest that the first solvation shell of Ca^+ may be filled up with ~6 water molecules, as opposed to Mg^+ which is saturated with 3 water molecules.[27] We are aware of one more gas phase mass spectrometry study reporting water detachment energies for $Ca(H_2O)_{1\text{-}5}^+$.[45]

From the theoretical side, little is known about the geometric and electronic structure of the calcium water clusters. The Monte Carlo simulations of Kochanski and Constantin for $Ca(H_2O)_{1\text{-}10}^+$ suggest that the first solvation shell fills up with six water molecules, and that the most stable structure for $Ca(H_2O)_{6\text{-}10}^+$ has a $Ca(H_2O)_6^+$ core.[45] Their statistically averaged coordination number for $Ca(H_2O)_6^+$ is 5.29 indicating that arrangements with a $Ca(H_2O)_5^+$ core and one H_2O in the second solvation shell are also encountered. This average coordination number increases to 5.63 for $Ca(H_2O)_{10}^+$. The later work of Watanabe and Iwata, however, suggests that the lowest energy structure of $Ca(H_2O)_6^+$ has a $Ca(H_2O)_4^+$ core with two hydrogen bonded water molecules, with the hexa-coordinated complex to be 13.65 kcal/mol higher (free energy at room temperature).[46] Bauschlicher *et al.* studied the smallest three clusters, $Ca(H_2O)_{1\text{-}3}^+$ reporting water detachment energies. Given that all of these studies are at the Hartee-Fock level, a more accurate and systematic theoretical investigation is necessary. Presently, we examine the lowest energy structures at the second-order Møller–Plesset perturbation theory (MP2) level of theory.

For specific n values, $M(H_2O)_n$ or $M(NH_3)_n$ systems can be pictured as a solvent separated electron from a metal-ammonia or metal-water core, $qe^-@M(H_2O/NH_3)_n^{q+}$. We named such species solvated electron precursors (SEPs).[35] $Be(NH_3)_4$ is our first reported SEP, where two electrons rest in the periphery of $Be(NH_3)_4^{2+}$.[47] The two outer electrons (q=2) of $Be(NH_3)_4$ occupy a diffuse s-type orbital in the ground state and can be promoted to higher energy hydrogenic type orbitals. Specifically, the outer electron of excited $Be(NH_3)_4^+$ populates (in energy order) the 1p, 1d, 2s, 1f, 2p, 2d orbitals. A similar shell model has been observed for $Li(NH_3)_4$, $Na(NH_3)_4$, and $Ca(NH_3)_8$ species.[35, 48] We also discovered that transition metal ammonia complexes, $Sc(NH_3)_6$, $V(NH_3)_6$ and $Y(NH_3)_8$ behave as SEPs.[49-51] In $Sc(NH_3)_6$ and $V(NH_3)_6$, in addition to the peripheral orbitals, one and three inner d-electrons remain in the t_{2g} and/or e_g orbitals.[50, 51] On the other hand, all $5s^2 4d^1$ valence electrons of Y solvate in the periphery of $Y(NH_3)_8$.[49] Recently, we reported our first H_2O-based SEPs, $Be(H_2O)_4^{0,+}$ and $Mg(H_2O)_6^{0,+}$.[52] We were able to expand the previously introduced Aufbau principle for SEPs beyond the 2d shell exploiting its higher D_{2h} symmetry. In the ground state of $Mg(H_2O)_6^+$ and $Mg(H_2O)_6$ one and two outer electron(s) occupy a quasi s-orbital.[52] The outer electron of $Mg(H_2O)_6^+$ can advance to one of the 1p, 1d, 2s, 2p, 1f, 2d, 3s, or 1g outer orbitals in energy order.[52] The observed series of $Mg(H_2O)_6^+$ is slightly different from that of $Be(NH_3)_4^+$. The first four shells are identical in both $Mg(H_2O)_6^+$ and $Be(NH_3)_4^+$, but 1f of the former falls in between 2p and 2d, and it rests in between 2s and 2p in the latter.[47, 52]

The present report is devoted to the characterization of the geometric and electronic structure of the $Ca(H_2O)_n^{+,0}$ (n=1–8) species, and are compared with the corresponding magnesium-water and calcium-ammonia species.[48, 52] We focus on the more symmetric hexa- and octa-coordinated complexes, which can be characterized as SEPs, and investigate their excited states. Do these systems follow the same Aufbau principle introduced for $Mg(H_2O)_6^+$? How will the excitation energies be affected going from Mg to Ca or from hexa- to octa-coordinated complexes or from water to ammonia complexes? To answer these questions, we have performed high-level quantum calculations and our findings are discussed in this article. In addition, we see the effect of a second shell of H_2O molecules on the excitation energies for a SEP such as $Ca(H_2O)_6@12H_2O^+$ and compare with our recent findings on $M(NH_3)_4@12NH_3$, M = Li, Be^+, B^{2+}.[53]

2. Computational details

Initially, we optimized the lowest energy structures for $[Ca,nH_2O]^+$ (n=1-7) at the MP2 level of theory using aug-cc-pVTZ basis sets[54-56] for all atoms and correlating all valence electrons. The diffuse functions for calcium were obtained by multiplying the smallest exponents of each shell of cc-pVTZ by 0.3. The diffuse functions on hydrogen and oxygen are needed for the accurate description of possible hydrogen bonds and the diffuse outer orbitals of SEPs. Two kinds of structures are considered, these with all water molecules attached directly to calcium denoted as $Ca(H_2O)_n^+$, and these with a number (k) of water molecules hydrogen bonded to the first solvation shell water ligands denoted as $Ca(H_2O)_n@kH_2O^+$. For the $Ca(H_2O)_{1\text{-}8}^{+,0}$ species, we performed additional calculations correlating the sub-valence $2s^22p^63s^23p^6$ electrons of Ca as well (C-MP2). The core-valence cc-pCVTZ basis set for Ca,[57] the cc-pVTZ for O, and the aug-cc-pVTZ for H were used in this case.

Harmonic vibrational frequencies were obtained at the Density Functional Theory (DFT/B3LYP) level of theory for the $Ca(H_2O)_{n=0\text{-}8}^{0,+}$ complexes using the cc-pVTZ(Ca,O) and aug-cc-pVTZ(H) basis set. The structures were re-optimized at B3LYP starting from the corresponding optimal MP2 structures. Frequency calculations confirmed the stability of the structures and are used to obtain zero-point energies (ZPE). For the relative MP2 energetics of the $Ca(H_2O)_n$ and $Ca(H_2O)_m@kH_2O$ structures of Figures 1 and 4, the ZPE and free energy corrections are calculated with MP2/aug-cc-pVTZ harmonic vibrational frequencies.

$Ca(H_2O)_6$ bears no symmetry rendering the multi-reference excited state calculations impractical. To provide excitation energies, we optimized the $Ca(H_2O)_6$ under C_s symmetry and used this geometry to calculate vertical excitations. The C_s structure of $Ca(H_2O)_6$ is 1.10 kcal/mol higher than its C_1 minimum at the MP2 level of theory. The first excitation energy at MP2 under C_1 and C_s symmetry are 0.64 and 0.60 eV, respectively. Therefore, we believe that the accuracy of our vertical excitation energies is affected by the constrained C_s optimization by less than 0.1 eV. We have used the original D_{2h} structure of $Ca(H_2O)_6^+$ to obtain its vertical excitation energies. Both $Ca(H_2O)_8^+$ and $Ca(H_2O)_8$ have S_8 symmetry. We have used their largest abelian sub-point group, C_2, for the excited state calculations. All optimized structures, their energies, and their frequencies are listed in the Electronic Supplementary Information (ESI).

Vertical excitation energies for $Ca(H_2O)_{6,8}^+$ were studied at CASSCF and CASPT2 levels of theory. A single active electron is allocated in 35 ($10a_g$, $4b_{3u}$, $4b_{2u}$, $4b_{1g}$, $4b_{1u}$, $4b_{2g}$, $4b_{3g}$, $1a_u$) and 9 (5a, 4b) active orbitals for $Ca(H_2O)_6^+$ and $Ca(H_2O)_8^+$ CASSCF calculations, respectively. For the calculations of $Ca(H_2O)_6$ and $Ca(H_2O)_8$, two active electrons are distributed in 9 (6a′, 3a′′ and 5a, 4b) active orbitals, respectively. CASPT2 calculations were performed on top of the CASSCF wave function and correlating all electrons except $1s^22s^22p^63s^23p^6$ of Ca and $1s^2$ of O. We have also performed C-CASPT2 calculations, where all electrons except $1s^2$ of Ca and O are correlated, for the $Ca(H_2O)_6^+$ and $Ca(H_2O)_8^+$ species. For the CASPT2 and C-CASPT2 calculations, the corresponding MP2 and C-MP2 structures were utilized. Unless otherwise stated, excitation energies are calculated with the following basis sets: cc-pVTZ or cc-pCVTZ (Ca) for CASPT2 or C-CASPT2, and cc-pVTZ (O), d-aug-cc-pVTZ (H) for both. A doubly diffuse basis set on hydrogenic centers suffices to provide excitations energies with better than 0.1 eV accuracy.[47]

Excitation energies of $Ca(H_2O)_6^+$ and $Ca(H_2O)_8^+$ systems were also studied using the EOM-EA-CCSD method.[58] For the $Ca(H_2O)_6^+$ we used two series of basis sets, a small double-ζ quality [cc-pVDZ (Ca), cc-pVDZ (O), d-aug-cc-pVDZ (H)] and a bigger triple-ζ quality [cc-pVTZ (Ca), cc-pVTZ (O), d-aug-cc-pVTZ (H)]. We show that the results with the two basis sets are in remarkable agreement. Therefore, due to the technical difficulties the $Ca(H_2O)_8^+$ was only studied with the small cc-pVDZ (Ca), cc-pVDZ (O), d-aug-cc-pVDZ (H) basis set. Furthermore, the excited states of $Ca(H_2O)_6^+$ and $Ca(H_2O)_8^+$ species were investigated through the partial third-order quasiparticle (P3+) electron propagator method[59, 60] and core-P3+ (C-P3+) levels of theory using cc-pVTZ (Ca)/cc-pCVTZ (Ca), cc-pVTZ (O), d-aug-cc-pVTZ (H) basis set. For the C-P3+ calculations we correlated all electrons except $1s^2$ of Ca and O.

The $Ca(H_2O)_6@12H_2O^+$ structure was optimized at CAM-B3LYP/aug-cc-pVTZ under constrained S_6 symmetry (the highest abelian group is C_i). We recently showed that CAM-B3LYP provides geometries with MP2-level accuracy for similar systems.[53] There is no strong evidence that this is the lowest energy structure, but the electronic structure and excitation energies are not expected to depend significantly on the orientation of the outer water molecules. The CAM-B3LYP optimized geometry was used to study the excited states of the system with CASSCF, MP2, D2, and P3+. The CASSCF wave-function consists of one electron in 9 active orbitals ($6a_g$, $3a_u$). We used d-aug-cc-pVDZ basis set for all H atoms and cc-pVDZ basis set for Ca and O. Several electronic states of $Ca(H_2O)_6@12H_2O^+$ were studied with MP2, where the use of d-aug-cc-pVTZ for H atoms and cc-pVTZ for the rest atoms was feasible. The excited states were finally investigated using the diagonal second-order approximation (D2) and P3+ methods.[59, 60] We introduced the d-aug-cc-pVDZ (H), cc-pVDZ (Ca,O) basis set (dADZ) in both D2 and P3+ calculations. For D2, the use of the d-aug-cc-pVTZ (H), cc-pVTZ (Ca,O) basis set (dATZ) combination was also possible. To get an estimate of the P3+ values with the triple-ζ basis set, we added the difference of the D2 excitation energies (ΔE) between the two basis sets to the P3+ double-ζ values. This quasi-P3+/dATZ method is reported as qP3+:

$$\Delta E(qP3+) = \Delta E(P3+/dADZ) + \Delta E(D2/dATZ) - \Delta E(D2/dADZ)$$

Gaussian16 suite was used to perform geometry optimizations and frequency calculations,[61] MOLPRO 2015.1 was implemented to carry out multi-reference calculations,[62] and QChem was invoked for the EOM-EA-CCSD calculations.[63]

3. Results and Discussion

3A. Cationic complexes

Ground state of $Ca(H_2O)_{n=1-8}^+$. According to the Hartree-Fock work of Watanabe and Iwata, the first four water molecules bind directly to the calcium center,[46] while one to three more water molecules stay in the second solvation shell attaching to the first four with hydrogen bonds. Interestingly, the addition of one more water molecule (totally eight) leads to a penta-coordinated calcium complex. These results are in contrast with our MP2 calculations, which indicate that the first five water molecules bind directly to calcium. The sixth molecule stays in the second solvation shell, $Ca(H_2O)_5@H_2O^+$, with the hexa-coordinated complex being higher by less than 1 kcal/mol after correcting for ZPE. The addition of a seventh water molecule stabilizes the $Ca(H_2O)_6^+$ core. The most stable structure is $Ca(H_2O)_6@H_2O^+$ with the $Ca(H_2O)_7^+$ isomer being 1.5 kcal/mol higher in energy (ZPE applied). All of these structures along with their relative energetics are shown in Figure 1. The structures reported with one or two water molecules in the second solvation shell form at least two hydrogen bonds with the first-shell water ligands. According to our calculations, these are the lowest energy isomers. Notice that structures with two or more water molecules in the second solvation shell are less stable, and that ZPE and free energy corrections at 20 °C and 1 atm favor the $Ca(H_2O)_n^+$ (n water ligands attached to calcium) ions. Our findings are in agreement with the Monte Carlo study of Kochanski and Constantin (see Section 1), who suggested that $Ca(H_2O)_6^+$ complexes dominate in solution phase. These observations are different from calcium ammonia complexes, where the first eight molecules for the (more weakly bound) neutral species bind directly to calcium.[48, 64]

Presently we investigate further both the hexa- and octa-coordinated water species for comparison with ammonia. Although, the geometric structure for calcium water complexes has been studied in the literature, their electronic structure remains largely unknown. Our calculations indicate that there is the Ca^+ center present for the smaller species becomes a Ca^{2+} center and an unpaired electron is displaced in the periphery of the $Ca(H_2O)_{n=6\text{-}8}{}^{2+}$ skeleton. Figure 2 shows the contour for the orbital of this unpaired electron. Every additional water ligand "pushes" away this electron from the valence space of calcium more and more.

Table 1 lists the detachment energies (D_e) of one water molecule from the $Ca(H_2O)_n^+$ species (all n water ligands attached to calcium). D_e MP2 values start from 20.7, 20.8 kcal/mol for n = 1, 2 and gradually reduce to 17.3 kcal/mol for n = 5. There is a sudden drop for n = 6 to 10.9 kcal/mol. Interestingly, D_e increases for n = 7 back to 17.1 kcal/mol and for n = 8 decreases again to 11.5 kcal/mol. The interaction energy (hydrogen bonding) between a second- and first-shell water molecule is around 14 kcal/mol, calculated as the average of the MP2 energy differences between $Ca(H_2O)_{1,4,5}@H_2O^+$ and $Ca(H_2O)_{1,4,5}^+$ (at the geometry of $Ca(H_2O)_{1,4,5}@H_2O^+$) + H_2O (13.1, 14.1, 15.1 kcal/mol, respectively). This interaction is stronger than the H_2O-$Ca(H_2O)_5$ binding. Considering that the hydrogen bonding interactions are slightly affected by the nature of the first coordination sphere, the two numbers (10.9 vs. ~14 kcal/mol) can explain why the sixth water balances between the first and second solvation shell. The hydrogen bonding interaction between a second- and first-shell weakens considerably after the inclusion of ZPE (6.6 kcal/mol for $Ca(H_2O)_{@}H_2O^+$), which rationalizes why ZPE favors the $Ca(H_2O)_n^+$ over $Ca(H_2O)_{n-k}@kH_2O^+$ complexes.

The core electron correlation effect enhances the binding energy by up to 5.7 kcal/mol (n = 1). The second larger increase belongs to n = 6 (4.9 kcal/mol), while the increase is smaller than 3.2 kcal/mol for the rest species and actually negative (-0.4 kcal/mol) for n = 8. Finally, ZPE reduces the detachment energies by up to 2.2 kcal/mol (n = 7). Our final D_0 values at C-MP2 compare favorably with the experimental data of ref. [45] with an average discrepancy of 1.7 kcal/mol (our values are always smaller); see Table 1. Table 1 reveals also that C-MP2 shortens appreciably the Ca-O distances (~0.1 Å).

Comparing calcium-water, magnesium-water,[52] and calcium-ammonia[48] complexes, we see that C-MP2 predicts comparable D_0 energies for all cases and n = 2 – 6. There is no specific trend going from Mg to Ca; for n = 2, 3, 6 values Mg-water binding energies are larger and for n = 4, 5 Ca-water ones are larger. The differences are within 3.2 kcal/mol. Ca-ammonia binding energies are always larger by 1.3 kcal/mol on average over all n = 2 – 6 values. These observations indicate that neither the identity of the metal nor the nature of the ligand plays an important role to the stability of the coordination complexes.

Excited states of $Ca(H_2O)_{6,8}^+$. In this section we study the excited states of the dominant (in condensed phase or bigger clusters) $Ca(H_2O)_6^+$ species. The $Ca(H_2O)_8^+$ is also studied as the largest complex with all ligands attached to the metal. Tables 2 and 3 collect the vertical excitation energies at different methodologies including CASSCF, CASPT2, P3+, and EOM-EA-CCSD. Figure 3 depicts the contours of representative orbitals populated in the low-lying electronic states of $Ca(H_2O)_6^+$; those of $Ca(H_2O)_8^+$ have identical morphology.

The ground state in both cases has a $1s^1$ configuration, which is followed by the $1p^1$, $1d^1$, $2s^1$, $1f^1$, $2p^1$, $1g^1$, $3s^1$ states. The expected degeneracy for states with same configuration is lifted because of the lower symmetry of the complexes compared to hydrogen atom. The T_h point group of $Ca(H_2O)_6^+$ keeps the degeneracy of p-type orbitals, but splits the d-orbitals to the e_g and t_g groups, the f-orbitals to a_u, and two t_u groups, and the g-orbitals to a_g, e_g, and two t_g groups. The S_8 point group of $Ca(H_2O)_8^+$ allows up to doubly degenerate groups (see Table 3).

Focusing on the excitation energies of $Ca(H_2O)_6^+$ and how the different methods perform, we make the following comments. The low CASSCF values by 0.5 eV in some cases (compared to CASPT2) indicate that dynamic electron correlation is certainly important. The dynamic correlation coming from the sub-valence electrons of calcium generally increase our values on average by only 0.05 eV (CASPT2 vs. C-CASPT2) or 0.01 eV (P3+ vs. C-P3+). Our values seem to be highly insensitive to the level of dynamic electron correlation treatment.

Due to the high symmetry of $Ca(H_2O)_6^+$, the three 1p and three 2p components are degenerate. The smallest range of excitation energies within the d, f, and g-type states belongs to $2d^1$ (2^2E_g and 2^2T_g). The components of 1d, 1f, and 1g of $Ca(H_2O)_6^+$ are within 0.39, 0.37, and 0.44 eV at CASPT2, but that of the more diffuse 2d is only 0.01 eV. For $Ca(H_2O)_8^+$, The P3+ splitting for the 1p, 1d, and 1f states is 0.30, 0.39, and 0.28 eV, but that of 2p is only 0.09 eV. The smaller splitting of 2d and 2p is because these orbitals have an additional node compared to the 1p, 1d, 1f, or 1g orbitals, expand further in space, and experience the $Ca(H_2O)_{6,8}^{2+}$ core more as an isotropic structure.

Next, we compare the weighted (according to degeneracy) averaged P3+ excitation energies of the states studied in common for the two species. The excitation energies for 1p, 1d, 2s, 1f, and 2p are (n = 6/8) 0.93/0.81, 1.92/1.70, 2.69/2.55, 3.03/2.61, and 3.11/2.92 eV, respectively. The excitation energies are always lower for n = 8 by at least 0.12 eV as expected due to the more diffuse nature of the outer electron of $Ca(H_2O)_8^+$. Very similar observations were made for the $Ca(NH_3)_{6-8}^+$ sequence.[48] Finally, the excitation energies of the $Ca(H_2O)_6^+$, $Mg(H_2O)_6^+$, and $Ca(NH_3)_6^+$ for the different states agree within 0.2 eV (compare present Table 2 with Tables 2 of refs. [52] and [48]). The excitation energies are generally higher for $Mg(H_2O)_6^+$, but no obvious trend is observed between the calcium water and ammonia complexes.

3B. Neutral complexes

***Ground state of Ca(H_2O)$_{n=1\text{-}8}$*.** No experimental or theoretical information is found in the literature about the stability and structure of the neutral calcium water complexes. To this end, we first optimized the geometry of the complexes from two to six water molecules. Besides the complexes with all water ligands coordinated to calcium, $Ca(H_2O)_n$, we also considered the complexes with one water molecule hydrogen bonded to one of the first coordination sphere water ligands, $Ca(H_2O)_n$@H_2O. Compared to cationic complexes, the presence of a second electron in the valence shell of calcium is expected to further deter water ligands from binding to calcium. Indeed, the binding energies are smaller and the equilibrium Ca-O distances longer by ~0.1 Å (see Table 1).

At the same time, the placement of a water ligand to the second coordination sphere is also less favorable for the neutral systems. For example, the neutral $Ca(H_2O)_5$ and $Ca(H_2O)_6$ complexes are more stable than $Ca(H_2O)_4$@H_2O and $Ca(H_2O)_5$@H_2O by 1.5 and 1.7 kcal/mol (ZPE corrected values; see Table 4) as opposed to the cations where the latter structures are slightly more stable (compare Figures 1 and 4). Free energy corrections at 20 ^oC and 1 atm make little difference from ZPE corrected values. Actually they favor further $Ca(H_2O)_5$. The $Ca(H_2O)_n$ and $Ca(H_2O)_{n-1}$@H_2O isomers are practically isoenergetic for n=2 with or without the ZPE/free energy correction, while their energy difference for n=3 is completely inverted when ZPE/thermal corrections are included (see Figure 4). For n=3-6, ZPE corrections clearly favor the $Ca(H_2O)_n$ structure. These observations indicate that going from the cationic to the neutral species the Ca-water interaction becomes weaker not only for the directly connected (to Ca) water ligands, but also for the second sphere water molecules. Actually, the latter interactions attenuate faster enhancing the stability of the $Ca(H_2O)_n$ species.

Focusing on the $Ca(H_2O)_n$ complexes, the attachment of a water molecule to calcium stabilizes the system by 5.7-11.2 kcal/mol at MP2. This range becomes 7.1-14.8 kcal/mol at C-MP2 and 7.0-14.3 kcal/mol when ZPE is added (see Table 1). Interestingly, the binding energy of the additional water is increasing, albeit only slightly, for bigger complexes in contrast with the cationic species where the binding energy decreases with the size. On the other hand, in both cationic and neutral species the sub-valence electron correlation (C-MP2) shortens the Ca-O bond lengths by ~0.1 Å.

Excited states of Ca(H_2O)$_{n=6,8}$. The binding energies for the larger neutral complexes are smaller, but still comparable to the energies of the experimentally observed cationic complexes (see Table 1) and these of the experimentally observed neutral calcium-ammonia complexes.[64] Ca(H_2O)$_6$ is the smallest complex where the electronic density of the two valence electrons is evenly distributed in the periphery of the Ca^{2+}(H_2O)$_6$ core (see Figure S1 of the SI), and can be characterized as an SEP. We presently study the excited states of Ca(H_2O)$_6$, as well as the highly-symmetric Ca(H_2O)$_8$ complex.

The ground state of both systems has $1s^2$ configuration, which is followed by the three $1s^11p^1$ components of triplet spin multiplicity. These correspond to two $^3A'$ and one $^3A''$ states (C_s symmetry) for Ca(H_2O)$_6$, and to ^3B and $^3E_1$ states (S_8 symmetry) for Ca(H_2O)$_8$. The analogous ^3P atomic term is listed in Table 4 along with the range of CASPT2 excitation energies of 0.60-0.92 eV and 0.33-0.69 eV for Ca(H_2O)$_6$ and Ca(H_2O)$_8$, respectively. The corresponding CASSCF excitation energies are 0.10-0.24 eV lower as happens for the cationic systems. Additionally, the excitation energies drop going from Ca(H_2O)$_6$ to Ca(H_2O)$_8$. The same effect was observed for Ca(NH_3)$_{6,8}$ and was attributed to the more diffuse electronic density in the case of the octa-coordinated complex.[48] The more distant (from the Ca^{2+} core) electrons of Ca(NH_3)$_8$ can easier be excited or removed. Specifically, the 1st ionization energy of Ca(NH_3)$_6$ and Ca(NH_3)$_8$ are 3.43 eV and 3.24 eV, respectively.

The next states are of both singlet and triplet spin multiplicities. The triplets have pure $1p^2$ (^3P) and $1s^11d^1$ (^3D) configurations, while the singlets are of heavily mixed character mingling the $1s^11p^1$ (^1P), $1p^2$ (^1D), and $1s^11d^1$ (^1D) configurations. The energy order is unclear for the different groups of components, and a detailed list of the calculated energy spectrum is provided in the SI. Generally, the excitations are lower in energy for octa-coordinated species, and the order of ^3D and ^3P groups is reverse for the two complexes.

3C. Dual solvation shell species

The consideration of a second solvation shell of water molecules for the $Ca(H_2O)_6^+$ complex is the topic of this section. Similar theoretical studies have been reported for transition metal cations with oxidation states (2+ or 3+)[65, 66] that do not afford an outer electron, as opposed to Ca^+. Although the $Ca(H_2O)_5@H_2O^+$ isomer is more stable for the [Ca,6H_2O] system by just 0.8 kcal/mol (see Figure 1), the addition of more water molecules will stabilize the $Ca(H_2O)_6^{2+}$ core as happens for the Mg-water complexes.[28] Therefore, we extended our study to the $Ca(H_2O)_6@12H_2O^+$ complex to see the effect of the second solvation shell for a water complex, as we did recently for the $M(NH_3)_4@12NH_3$ ammonia complexes with M = Li, Be^+, and B^{2+}.[53] The optimized structure was obtained at the CAM-B3LYP level (see Figure 5) and the excitations energies with various electronic structure approaches (see Table 5). The obtained $Ca(H_2O)_6@12H_2O^+$ polyhedron has S_6 symmetry.

The large computational cost allowed us to explore only the $1s^1$, $1p^1$, and $1d^1$ electronic states. For the calculation of their excitation energies we employed the CASSCF (practically Hartree-Fock), MP2, D2, and P3+ methodologies combined with either double- or triple-ζ basis sets. The calculated excitation energies seem largely insensitive to the method or basis set used, except for the dynamic-correlation-free CASSCF level. Specifically, the highest deviation of 0.07 eV in the relatively high energy $2^2E_g(1d^1)$ state. As in the $Ca(H_2O)_6$ complex, the first excited state is of $1p^1$ character. However, the three components are not triply degenerate any more due to the anisotropy of the $Ca(H_2O)_6@12H_2O^+$ polyhedron, with the relative 1^2E_u and 1^2A_u states being separated by ~0.33 eV (see Table 5). Similarly, the next five $1d^1$ components are grouped as 1^2E_g, 2^2E_g, and 2^2A_g covering a range of about 0.45 eV. Overall, the $1p^1$ and $1d^1$ states lie at 0.33-0.66 (weighted average 0.44) and 0.82-1.26 (weighted average 0.97) eV, respectively, at the composite qP3+ level of theory. The corresponding P3+ numbers for $Ca(H_2O)_6$ are 0.93 and 1.69-2.07 (weighted average 1.92) eV (see Table 2), about double of the previous numbers.

4. Conclusions

Presently we performed high level quantum chemical calculations to characterize the geometric and electronic structure of cationic and neutral calcium water complexes. Neutral complexes favor the coordination of water ligands directly to the metal more than the corresponding positively charged complexes. For example, $Ca(H_2O)_6$ is more stable than $Ca(H_2O)_5@H_2O$, but $[Ca,6H_2O]^+$ composition prefers $Ca(H_2O)_5@H_2O^+$. The $Ca(H_2O)_6^+$ core is formed however for $[Ca,7H_2O]^+$. The dissociation of a water molecule is easier for neutral species, and especially for the smaller of them. The dissociation of a water ligand for cations is easier for the bigger members. For six or more water ligands, the valence calcium electrons are displaced to the periphery of the complex as has been previously observed for a series of species called SEPs.

The energy pattern for the excited states of the "one-electron" $Ca(H_2O)_{6,8}^+$ follows the same Aufbau principle observed for the previously reported SEPs: 1s, 1p, 1d, 2s, 1f, 2p, 2d, 1g, 3s. The excitation energies drop going from the hexa- to the octa-coordinated complexes as expected because the electronic density of the latter is more remote from the metal center. Compared to magnesium water and calcium ammonia complexes, the excitation energies follow the order Mg-water > calcium-water ~ calcium ammonia. The electronic spectrum of the neutral complexes is quite complex with the relative excited states being of multi-reference nature. Finally, we saw that a second solvation shell of water molecules around $Ca(H_2O)_6^+$ reduces the excitation energies by a factor of almost two.[47, 53]

Our findings are expected to benefit future experimental studies aiming at the elucidation of the geometric and electronic structure of the calcium water complexes.

Conflicts of interest

There are no conflicts to declare

Acknowledgements

The authors are indebted to Auburn University (AU) for financial support. This work was completed with resources provided by the Auburn University Hopper Cluster, Alabama Supercomputer, and the National Energy Research Scientific Computing Center, a DOE Office of Science User Facility supported by the Office of Science of the U.S. Department of Energy under Contract No. DE-AC02-05CH11231. This material is based upon work supported by the National Science Foundation under Grant No. CHE-1940456. Any opinions, findings, and conclusions or recommendations expressed in this material are those of the author(s) and do not necessarily reflect the views of the National Science Foundation.

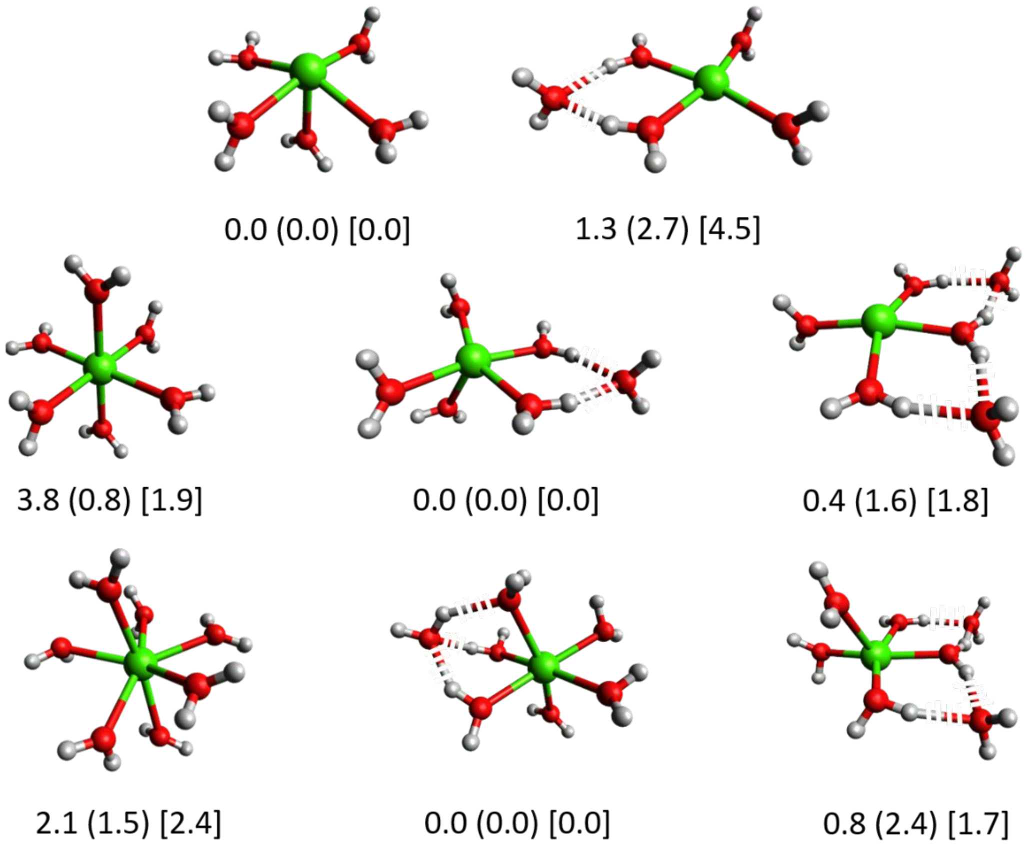

Figure 1. MP2/aug-cc-pVTZ relative energies (kcal/mol) for the more stable structures of positively charged calcium water species with five to seven water molecules. ZPE-corrected and free energy corrected (at 20 °C temperature and 1 atm pressure) values (using MP2 frequencies) are shown in parenthesis and square brackets, respectively; CAM-B3LYP frequencies are used for seven water molecules.

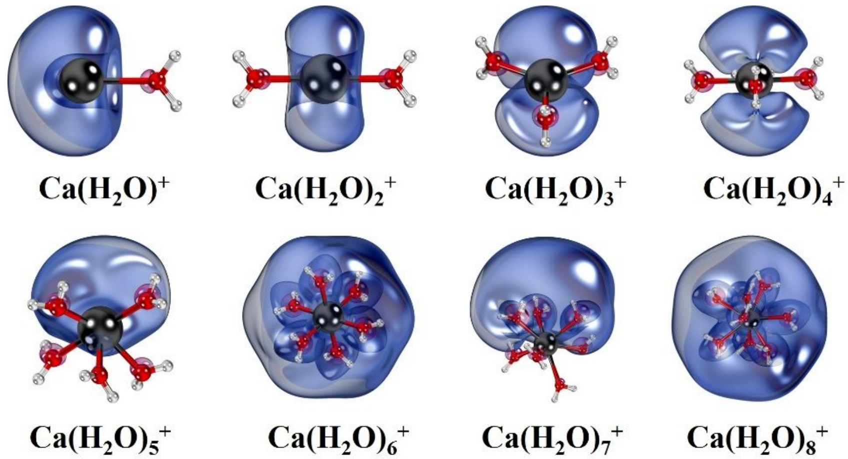

Figure 2. Contours of the highest (singly occupied) occupied molecular orbital of $Ca(H_2O)_{n=1\text{-}8}^+$ for their doublet ground state.

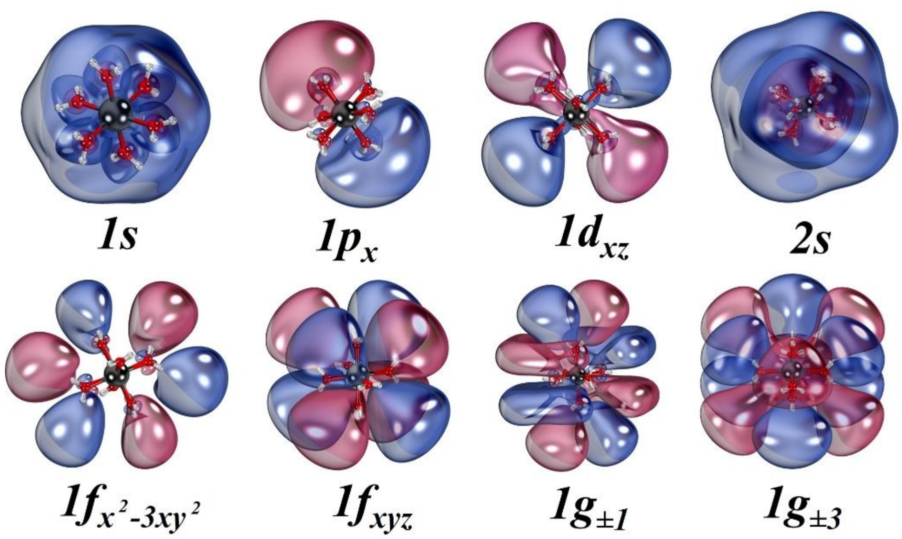

Figure 3. Selected outer orbitals of $Ca(H_2O)_6^+$.

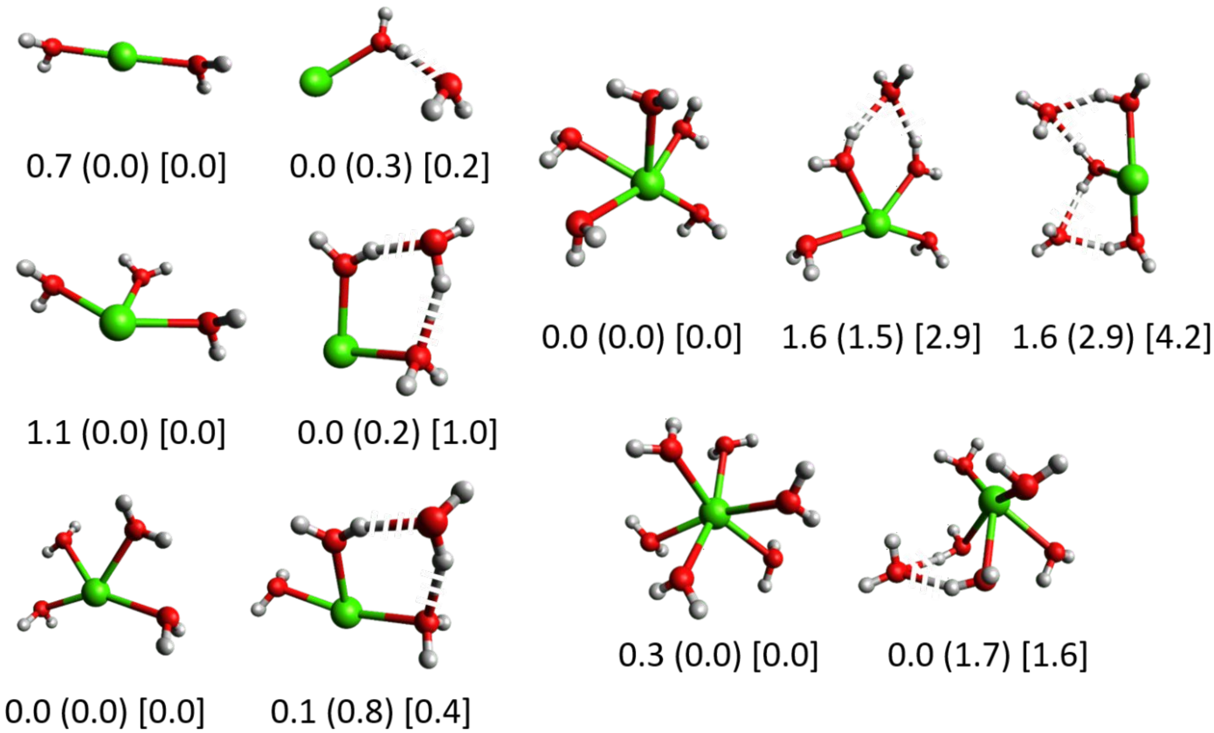

Figure 4. MP2/aug-cc-pVTZ relative energies (kcal/mol) for the more stable structures of neutral calcium water species with two to six water molecules. ZPE-corrected and free energy corrected (at 20 ^{o}C temperature and 1 atm pressure) values (using MP2 frequencies) are shown in parenthesis and square brackets, respectively.

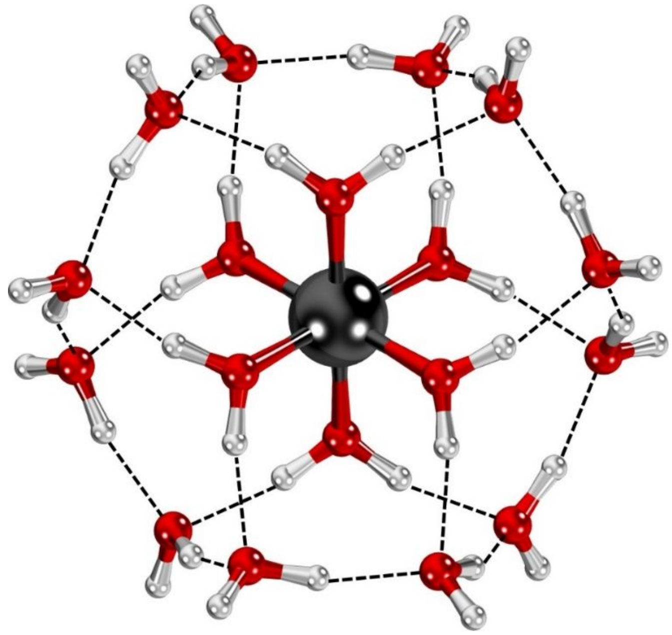

Figure 5. Optimized geometry of $Ca(H_2O)_6^+@12H_2O$. The dashed black lines show hydrogen bonds between water molecules.

Table 1. Average equilibrium Ca−O distances r_e (Å), and detachment energy of one water ligand D_e and D_0 (kcal/mol) for $Ca(H_2O)_{n=1\text{-}8}^{+,0}$ at MP2 and C-MP2 levels.[a]

	$Ca(H_2O)_n^+$						$Ca(H_2O)_n$				
	r_e		D_e [b]		D_0 [c]	Expt [d]	r_e		D_e [b]		D_0 [c]
n	MP2	C-MP2	MP2	C-MP2	C-MP2		MP2	C-MP2	MP2	C-MP2	C-MP2
1	2.452	2.344	20.7	26.4	25.3	28	2.565	2.431	5.7	7.1	7.0
2	2.448	2.348	20.8	24.0	22.9	24	2.506	2.389	7.0	9.6	9.1
3	2.458	2.354	16.5	19.0	18.1	21.5	2.518	2.420	8.9	10.4	10.0
4	2.476	2.380	17.4	18.6	17.7	18.7	2.541	2.421	10.3	11.9	11.1
5	2.501	2.404	17.3	17.6	17.3	17.5	2.555	2.425	10.1	13.1	14.3
6	2.442	2.367	10.9	15.8	15.4		2.504	2.401	10.1	13.4	11.1
7	2.529	2.421	17.1	19.2	17.0		2.500	2.431	13.1	14.8	12.2
8	2.517	2.448	11.5	11.1	9.8		2.521	2.455	11.2	10.8	9.1

[a] The basis set is cc-pVTZ(Ca) or cc-pCVTZ(Ca) for MP2 or C-MP2 and cc-pVTZ(O), aug-cc-pVTZ(H) for both methods.
[b] $D_e = E_e[H_2O] + E_e[Ca(H_2O)_{n-1}^{0,+}] - E_e[Ca(H_2O)_n^{0,+}]$, where E_e is the optimized equilibrium energy.
[c] $D_0 = E_0[H_2O] + E_0[Ca(H_2O)_{n-1}^{0,+}] - E_0[Ca(H_2O)_n^{0,+}]$, where $E_0 = E_e$ + ZPE(B3LYP/cc-pVTZ(Ca,O) and aug-cc-pVTZ(H)).
[d] Ref **26**.

Table 2. Electronic states, electronic configurations (Config.), and vertical excitation energies (eV) at CASSCF, CASPT2, C-CASPT2, P3+, C-P3+, and EOM-EA-CCSD of the first sixteen states of $Ca(H_2O)_6^+$.

State (T_h)	Config.	CASSCF (DATZ) [a]	CASPT2 (DATZ) [a]	C-CASPT2 (DATZ) [a]	P3+ (DATZ) [a]	C-P3+ (DATZ) [a]	EOM-EA-CCSD (DADZ) [b]	EOM-EA-CCSD (DATZ) [a]
1^2A_g	$1s^1$	0.00	0.00	0.00	0.00	0.00	0.00	0.00
1^2T_u	$1p^1$	0.76	0.97	1.04	0.93	0.95	0.96	0.98
1^2E_g	$1d^1$	1.50	1.74	1.73	1.69	1.71	1.74	1.74
1^2T_g	$1d^1$	1.72	2.13	2.12	2.07	2.10	2.15	2.18
2^2A_g	$2s^1$	2.34	2.73	2.76	2.69	2.70	2.76	2.80
2^2T_u	$1f^1$	2.44	2.86	2.92	2.79	2.82	2.86	2.89
1^2A_u	$1f^1$	2.61	3.09	3.08	3.06	3.09	3.13	3.14
3^2T_u	$1f^1$	2.76	3.23	3.29	3.25	3.27	3.27	3.30
4^2T_u	$2p^1$	2.67	3.16	3.22	3.11	3.13	3.18	3.23
2^2E_g	$2d^1$	3.12	3.59	3.59	3.52	3.55	3.60	3.66
2^2T_g	$2d^1$	3.17	3.60	3.73	3.59	3.60		
3^2T_g	$1g^1$	3.45	3.66	3.87	3.71	3.63		
3^2A_g	$1g^1$	3.49	3.99	4.00				
3^2E_g	$1g^1$	3.59	4.10	4.11				
4^2T_g	$1g^1$	3.65	4.05	4.16				
4^2A_g	$3s^1$	3.74						

[a] DATZ = cc-pVTZ (Ca,O), d-aug-cc-pVTZ (H).

[b] DADZ = cc-pVDZ (Ca,O), d-aug-cc-pVDZ (H).

Table 3. Electronic states, electronic configurations (Config.), and vertical excitation energies (eV) at CASSCF, CASPT2, C-CASPT2, P3+, C-P3+, and EOM-EA-CCSD of thirteen states of $Ca(H_2O)_8^+$.

State (S_8)	Config.	CASSCF (DATZ) [a]	CASPT2 (DATZ) [a]	C-CASPT2 (DATZ) [a]	P3+ (DATZ) [a]	C-P3+ (DATZ) [a]	EOM-EA-CCSD (DADZ) [b]
1^2A	$1s^1$	0.00	0.00	0.00	0.00	0.00	0.00
1^2E_1	$1p^1$	0.56	0.74	0.73	0.71	0.72	0.74
1^2B	$1p^1$	0.84	1.04	1.03	1.01	1.02	1.04
1^2E_2	$1d^1$	1.29	1.61	1.59	1.57	1.58	1.62
1^2E_3	$1d^1$	1.45	1.74	1.72	1.70	1.71	1.74
2^2A	$1d^1$	1.59	2.00	1.99	1.96	1.97	2.03
3^2A	$2s^1$				2.55	2.56	2.62
2^2E_3	$1f^1$				2.47	2.48	2.53
2^2E_2	$1f^1$				2.57	2.58	2.63
2^2E_1	$1f^1$				2.72	2.74	2.78
2^2B	$1f^1$				2.75	2.77	2.81
3^2E_1	$2p^1$				2.89	2.90	2.96
3^2B	$2p^1$				2.98	3.00	3.04

[a] DATZ = cc-pVTZ (Ca,O), d-aug-cc-pVTZ (H).

[b] DADZ = cc-pVDZ (Ca,O), d-aug-cc-pVDZ (H).

Table 4. Electronic configurations (Config.), electronic terms (State) and vertical excitation energies (eV) at CASSCF and CASPT2 for several low-lying states of $Ca(H_2O)_{6,8}$ at cc-pVTZ (Ca,O), d-aug-cc-pVTZ (H) basis set.

Config.	**State** [a]	**$Ca(H_2O)_6$**		**$Ca(H_2O)_8$**	
		CASSCF	CASPT2	CASSCF	CASPT2
$1s^2$	^1S	0.00	0.00	0.00	0.00
$1s^1 1p^1$	^3P	0.44-0.69	0.60-0.92	0.23-0.56	0.33-0.69
$1s^1 1d^1$	^3D	1.41-1.66	1.64-1.89	1.31-1.54	1.33-1.64
$1p^2$	^3P	1.71-2.00	1.98-2.29	0.99-1.21	1.21-1.43
$1s^1 1p^1/1s^1 1d^1/1p^2$	$^1P/^1D/^1D$	0.92-2.33	1.14-2.56	0.70-1.68	0.93-1.81

[a] The atomic terms corresponding to the assigned configuration is reported here. A more detailed list and the actual electronic terms are given in Tables S21 and S22 of the SI.

Table 5. Electronic terms, electronic configurations (Config.), and vertical excitation energies (eV) at the CASSCF, MP2, D2, and P3+ levels of theory for the first six states of $[Ca(H_2O)_6@12H_2O]^+$.

State (S_6)	**Config.**	**CASSCF (DADZ)** [a]	**MP2 (DATZ)** [b]	**D2 (DADZ)** [a]	**P3+ (DADZ)** [a]	**D2 (DATZ)** [b]	**qP3+ (DATZ)** [c]
1^2A_g	$1s^1$	0.00	0.00	0.00	0.00	0.00	0.00
1^2E_u	$1p^1$	0.24	0.35	0.32	0.32	0.33	0.33
1^2A_u	$1p^1$	0.46	0.70	0.65	0.65	0.66	0.66
1^2E_g	$1d^1$	0.64	0.86	0.80	0.80	0.82	0.82
2^2E_g	$1d^1$	0.75	1.03	0.96	0.96	0.98	0.98
2^2A_g	$1d^1$	0.94		1.22	1.23	1.25	1.26

[a] Basis set: cc-pVDZ (Ca,O), d-aug-cc-pVDZ (H).

[b] Basis set: cc-pVTZ (Ca,O), d-aug-cc-pVTZ (H).

[c] Quasi-DATZ. See Section 2.

References

1. E. Zurek, P. P. Edwards and R. Hoffmann, *Angewandte Chemie International Edition*, 2009, **48**, 8198-8232.
2. J. M. Herbert and M. P. Coons, *Annual Review of Physical Chemistry*, 2017, **68**, 447-472.
3. P. P. Edwards, *Journal of Superconductivity*, 2000, **13**, 933-946.
4. A. G. Seel, E. Zurek, A. J. Ramirez-Cuesta, K. R. Ryan, M. T. J. Lodge and P. P. Edwards, *Chemical Communications*, 2014, **50**, 10778-10781.
5. E. Zurek, X.-D. Wen and R. Hoffmann, *Journal of the American Chemical Society*, 2011, **133**, 3535-3547.
6. C. v. d. Linde and M. K. Beyer, *Physical Chemistry Chemical Physics*, 2011, **13**, 6776-6778.
7. M. Beyer, C. Berg, H. W. Görlitzer, T. Schindler, U. Achatz, G. Albert, G. Niedner-Schatteburg and V. E. Bondybey, *Journal of the American Chemical Society*, 1996, **118**, 7386-7389.
8. B. M. Reinhard and G. Niedner-Schatteburg, *The Journal of Physical Chemistry A*, 2002, **106**, 7988-7992.
9. C.-K. Siu, Z.-F. Liu and J. S. Tse, *Journal of the American Chemical Society*, 2002, **124**, 10846-10860.
10. M. Beyer, U. Achatz, C. Berg, S. Joos, G. Niedner-Schatteburg and V. E. Bondybey, *The Journal of Physical Chemistry A*, 1999, **103**, 671-678.
11. T. Tsurusawa and S. Iwata, *The Journal of Physical Chemistry A*, 1999, **103**, 6134-6141.
12. T. Tsurusawa and S. Iwata, *The Journal of Chemical Physics*, 2000, **112**, 5705-5710.
13. B. Gao and Z.-F. Liu, *The Journal of Chemical Physics*, 2007, **126**, 084501.
14. C. P. Schulz, R. Haugstätter, H. U. Tittes and I. V. Hertel, *Physical Review Letters*, 1986, **57**, 1703-1706.
15. C. P. Schulz, R. Haugstätter, H. U. Tittes and I. V. Hertel, *Zeitschrift für Physik D Atoms, Molecules and Clusters*, 1988, **10**, 279-290.
16. C. Steinbach and U. Buck, *Physical Chemistry Chemical Physics*, 2005, **7**, 986-990.
17. U. Buck and C. Steinbach, *The Journal of Physical Chemistry A*, 1998, **102**, 7333-7336.
18. C. J. Mundy, J. Hutter and M. Parrinello, *Journal of the American Chemical Society*, 2000, **122**, 4837-4838.
19. L. Bewig, U. Buck, S. Rakowsky, M. Reymann and C. Steinbach, *The Journal of Physical Chemistry A*, 1998, **102**, 1124-1129.
20. K. F. Willey, C. S. Yeh, D. L. Robbins, J. S. Pilgrim and M. A. Duncan, *The Journal of Chemical Physics*, 1992, **97**, 8886-8895.
21. F. Misaizu, M. Sanekata, K. Fuke and S. Iwata, *The Journal of Chemical Physics*, 1994, **100**, 1161-1170.
22. A. C. Harms, S. N. Khanna, B. Chen and A. W. Castleman, *The Journal of Chemical Physics*, 1994, **100**, 3540-3544.
23. T. Taxer, M. Ončák, E. Barwa, C. van der Linde and M. K. Beyer, *Faraday Discussions*, 2019, **217**, 584-600.
24. C. van der Linde, A. Akhgarnusch, C.-K. Siu and M. K. Beyer, *The Journal of Physical Chemistry A*, 2011, **115**, 10174-10180.
25. C. Berg, M. Beyer, U. Achatz, S. Joos, G. Niedner-Schatteburg and V. E. Bondybey, *Chemical Physics*, 1998, **239**, 379-392.
26. C. Berg, U. Achatz, M. Beyer, S. Joos, G. Albert, T. Schindler, G. Niedner-Schatteburg and V. E. Bondybey, *International Journal of Mass Spectrometry and Ion Processes*, 1997, **167-168**, 723-734.
27. Y. Inokuchi, K. Ohshimo, F. Misaizu and N. Nishi, *The Journal of Physical Chemistry A*, 2004, **108**, 5034-5040.

28. B. M. Reinhard and G. Niedner-Schatteburg, *The Journal of Chemical Physics*, 2003, **118**, 3571-3582.
29. C.-K. Siu and Z.-F. Liu, *Physical Chemistry Chemical Physics*, 2005, **7**, 1005-1013.
30. B. M. Reinhard and G. Niedner-Schatteburg, *Physical Chemistry Chemical Physics*, 2003, **5**, 1970-1980.
31. T.-W. Lam, C. van der Linde, A. Akhgarnusch, Q. Hao, M. K. Beyer and C.-K. Siu, *ChemPlusChem*, 2013, **78**, 1040-1048.
32. C. W. Bauschlicher, M. Sodupe and H. Partridge, *The Journal of Chemical Physics*, 1992, **96**, 4453-4463.
33. M. Ončák, T. Taxer, E. Barwa, C. van der Linde and M. K. Beyer, *The Journal of Chemical Physics*, 2018, **149**, 044309.
34. K. Hashimoto and K. Daigoku, *Physical Chemistry Chemical Physics*, 2009, **11**, 9391-9400.
35. I. R. Ariyarathna, F. Pawłowski, J. V. Ortiz and E. Miliordos, *Physical Chemistry Chemical Physics*, 2018, **20**, 24186-24191.
36. T. E. Salter, V. Mikhailov and A. M. Ellis, *The Journal of Physical Chemistry A*, 2007, **111**, 8344-8351.
37. S. Yoshida, K. Daigoku, N. Okai, A. Takahata, A. Sabu, K. Hashimoto and K. Fuke, *The Journal of Chemical Physics*, 2002, **117**, 8657-8669.
38. M. H. Shen and J. M. Farrar, *The Journal of Chemical Physics*, 1991, **94**, 3322-3331.
39. S. G. Donnelly and J. M. Farrar, *The Journal of Chemical Physics*, 1993, **98**, 5450-5459.
40. M. H. Shen, J. W. Winniczek and J. M. Farrar, *The Journal of Physical Chemistry*, 1987, **91**, 6447-6449.
41. D. C. Sperry, A. J. Midey, J. I. Lee, J. Qian and J. M. Farrar, *The Journal of Chemical Physics*, 1999, **111**, 8469-8480.
42. I. Cabanillas–Vidosa, M. Rossa, G. A. Pino and J. C. Ferrero, *Physical Chemistry Chemical Physics*, 2011, **13**, 13387-13394.
43. I. Cabanillas-Vidosa, M. Rossa, G. A. Pino, J. C. Ferrero and C. J. Cobos, *Physical Chemistry Chemical Physics*, 2012, **14**, 4276-4286.
44. M. Sanekata, F. Misaizu and K. Fuke, *The Journal of Chemical Physics*, 1996, **104**, 9768-9778.
45. E. Kochanski and E. Constantin, *The Journal of Chemical Physics*, 1987, **87**, 1661-1665.
46. H. Watanabe and S. Iwata, *The Journal of Physical Chemistry A*, 1997, **101**, 487-496.
47. I. R. Ariyarathna, S. N. Khan, F. Pawłowski, J. V. Ortiz and E. Miliordos, *The Journal of Physical Chemistry Letters*, 2018, **9**, 84-88.
48. I. R. Ariyarathna, N. M. S. Almeida and E. Miliordos, *The Journal of Physical Chemistry A*, 2019, **123**, 6744-6750.
49. N. M. S. Almeida and E. Miliordos, *Physical Chemistry Chemical Physics*, 2019, **21**, 7098-7104.
50. N. M. S. Almeida, F. Pawłowski, J. V. Ortiz and E. Miliordos, *Physical Chemistry Chemical Physics*, 2019, **21**, 7090-7097.
51. S. N. Khan and E. Miliordos, *The Journal of Physical Chemistry A*, 2020, **124**, 4400-4412.
52. I. R. Ariyarathna and E. Miliordos, *Physical Chemistry Chemical Physics*, 2019, **21**, 15861-15870.
53. I. R. Ariyarathna, F. Pawłowski, J. V. Ortiz and E. Miliordos, *The Journal of Physical Chemistry A*, 2020, **124**, 505-512.
54. T. H. Dunning, *The Journal of Chemical Physics*, 1989, **90**, 1007-1023.
55. R. A. Kendall, T. H. Dunning and R. J. Harrison, *The Journal of Chemical Physics*, 1992, **96**, 6796-6806.
56. D. E. Woon and T. H. Dunning, *The Journal of Chemical Physics*, 1994, **100**, 2975-2988.
57. J. Koput and K. A. Peterson, *The Journal of Physical Chemistry A*, 2002, **106**, 9595-9599.
58. M. Nooijen and R. J. Bartlett, *The Journal of Chemical Physics*, 1995, **102**, 3629-3647.

59. J. V. Ortiz, *International Journal of Quantum Chemistry*, 2005, **105**, 803-808.
60. J. V. Ortiz, *WIREs Computational Molecular Science*, 2013, **3**, 123-142.
61. M. J. Frisch, G. W. Trucks, H. B. Schlegel, G. E. Scuseria, M. A. Robb, J. R. Cheeseman, G. Scalmani, V. Barone, G. A. Petersson, H. Nakatsuji, et al. *Gaussian 16 Rev. B.01*, Wallingford, CT, 2016.
62. H.-J. Werner, P. J. Knowles, G. Knizia, F. R. Manby, M. {Schütz}, P. Celani, W. Györffy, D. Kats, T. Korona, R. Lindh, et al. *MOLPRO, version 2015.1, a package of ab initio programs*, 2015.
63. Y. Shao, Z. Gan, E. Epifanovsky, A. T. B. Gilbert, M. Wormit, J. Kussmann, A. W. Lange, A. Behn, J. Deng, X. Feng, et al. *Advances in molecular quantum chemistry contained in the Q-Chem 4 program package. [Mol. Phys. 113, 184–215 (2015)]*.
64. M. D. Albaqami and A. M. Ellis, *Chemical Physics Letters*, 2018, **706**, 736-740.
65. M. Radoń and G. Drabik, *Journal of Chemical Theory and Computation*, 2018, **14**, 4010-4027.
66. M. Radoń, K. Gąssowska, J. Szklarzewicz and E. Broclawik, *Journal of Chemical Theory and Computation*, 2016, **12**, 1592-1605.